Density-functional periodic study of the adsorption of hydrogen on a palladium (111) surface

J.-F. Paul and P. Sautet*
Institut de Recherche sur la Catalyse, CNRS, 2 Avenue A. Einstein, 69626 Villeurbanne Cedex, France
and Laboratoire de Chimie Théorique, Ecole Normale Supérieure, 69364 Lyon Cedex 07, France
(Received 31 July 1995)

The adsorption of H on Pd(111) has been studied with density-functional calculations both with local density approximation (LDA) and generalized gradient approximation (GGA) exchange-correlation functionals. The surface is described by a two-dimensional slab with a frozen or relaxed geometry and a periodic adsorption of H atoms is considered. Among the surface sites, the fcc hollow one is found to be the most stable, in agreement with other experimental and theoretical data. The GGA adsorption energy ranges from -0.27 to -0.53 eV (the experimental value is -0.45 eV) while the LDA result for the adsorption energy is 0.6–0.7 eV larger in absolute value. The optimal height of the H atom is $+0.85$ Å relative to the surface Pd layer, very close to the low-energy electron diffraction determination. The hcp hollow site is significantly less stable ($+0.15$ eV) than the fcc site and its binding energy is similar to that of the bridge site. The octahedral subsurface site is stable with respect to H_2, except for the frozen surface with a coverage 1. Indeed, if the surface is relaxed, the subsurface site is only 0.1 eV less stable than the fcc surface site. For the surface hollow site, the first to second layer Pd spacing expands when H is chemisorbed, but only by 2.7%. A larger expansion is found for the subsurface site. In the eigenvalue spectrum, a new peak is clearly visible below the Pd band when H is adsorbed and the position of that peak correlates with the H coordination. This surface state is mostly localized on the H and first layer Pd. The crystal orbital overlap population curves show that the predominant Pd-H bonding character is contained in the split-off band and indicate that the *sp* and *d* orbitals of Pd have a rather equal contribution to the Pd-H bond. The small surface relaxation is explained on the basis of the overlap population analysis.

I. INTRODUCTION

Transition metals from group 10 have always attracted a considerable amount of interest in heterogeneous catalysis, especially for the hydrogenation and dehydrogenation reactions. Among them, Pd is a very active metal for hydrogenation of unsaturated molecules and is also selective for partial hydrogenation of acetylene and butadiene,[1] which are important industrial reactions. Clearly, hydrogen is a key partner for these reactions and, considering its simplicity, the interaction of H with a transition-metal surface continues to attract a considerable amount of attention, both from the experimental and theoretical viewpoints.[2–5] The understanding of the geometric structure and electronic structure of H atoms on a transition-metal surface is of great importance for the determination of some elementary steps of the hydrogenation reaction. The ability of the H atom to diffuse on the surface[6–8] and, for Pd, in subsurface sites[9,10] is also of interest. This capability of Pd to form bulk phases with H, the solid solution or α phase and the hydride or β phase, has been an additional motivation for many studies and results in a rather large experimental data set for the (H,Pd) system.[11–13] Several theoretical studies have also appeared using semiempirical or first-principle techniques, since H is a good test case for chemisorption studies. Most of the first-principles calculations use a cluster to model the Pd surface.

We will concentrate here on the interaction of H atoms with the (111) surface of Pd. On that surface, H forms three superstructures:[2,14,15] a (1×1) structure and two phases with $(\sqrt{3}\times\sqrt{3})R30°$ symmetry, the first one containing 1 H per surface unit cell (coverage $\frac{1}{3}$) while the second one contains 2 H (coverage $\frac{2}{3}$). The second structure was studied by quantitative low-energy electron diffraction (LEED) analysis.[15] If only one type of site is supposed to be occupied on the surface (or below the surface) the surface fcc hollow site gives the best agreement (see Fig. 1 and Sec. III for a description of possible surface and subsurface adsorption sites). It should be noted that other possibilities of single site structures (including surface hcp hollow and subsurface fcc hollow) give significantly worse agreement. When a mixture of

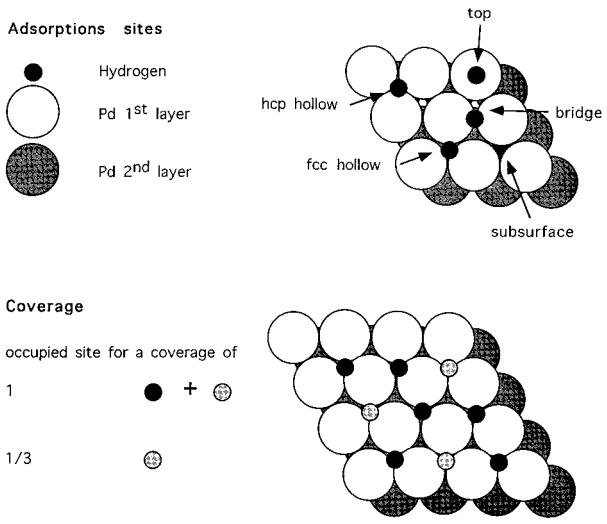

FIG. 1. Schematic description of the various adsorption sites and coverages for H on palladium (111) that were used in the calculations.

two sites is supposed, the best agreement is obtained when 20% of subsurface fcc sites are occupied with respect to the surface fcc sites. The different population and energy of surface hcp and fcc hollow sites is also suggested by helium diffraction[6] where a C_{3v} symmetry indicates a preferred occupation of 1 type of hollow site, without being able to tell which one.

The optimum Pd-H distance obtained by the LEED calculation for the surface fcc hollow site is 1.78 to 1.8 Å, which corresponds to a vertical height of 0.80–0.85 Å of H above the surface. For the subsurface hollow site, the H is found to be in the middle of the two Pd planes but shows a very large vertical disorder. The relaxation of the surface was also studied: for the clean surface the first layer shows a very small outward relaxation ($+0.025\pm0.05$ Å) and the H chemisorption (coverage $\frac{2}{3}$ only slightly increases this outward relaxation ($+0.03$ to $+0.05$ Å). The difficulty here is that the error bars are rather large (0.05 Å). Another LEED study[9] yields a 2% (0.05 Å) expansion of the first Pd interlayer spacing upon H adsorption. For the diffusion of H on Pd, only the bulk diffusion barrier is known experimentally[11] (0.23 eV) but suggests a small value for the surface diffusion barriers. The chemisorption energy of $\frac{1}{2}$ H_2 on Pd(111) has been measured by Conrad, Ertl, and Hata[16] to be 0.45 eV at low coverage. This energy is dependent on the coverage and reaches 0.4 eV near saturation.[17] When H is in the Pd bulk, the octahedral site is the most stable with an absorption energy of 0.2 eV.[13] There is no adsorption energy value for the subsurface site, even if there is some evidence that the concentration of H in the first layers might be larger than the one in the bulk. The vibrational states of H on Pd(111) have been studied by high-resolution electron energy loss experiments,[18] yielding $\omega=998$ cm^{-1} for the perpendicular mode of H on the surface site. This contrasts with the lower vibrational frequency of H in the Pd bulk (550 cm^{-1}).

In the present paper, a density-functional theoretical study of the absorption of H atoms on a Pd(111) surface is presented, both with a local [local density approximation (LDA)] and a nonlocal [generalized gradient approximation (GGA)] exchange-correlation functional. This system has already been studied with cluster models and first-principles LDA calculations,[19–21] but in that case the precise comparison of chemisorption sites and the determination of the energies is complicated by the dependence on the cluster shape and size. Embedded cluster models have also been applied to that system[22] but these calculations yield a preferred bridge site, in contrast with all other theoretical or experimental determinations. Periodic LDA calculations on that face have been performed by Louie and co-workers [23,24] but only for the analysis of the density of states and with no structural optimization. The comparison of the calculated results with experimental photoemission measurements,[25] however, shows that the H atoms prefer the hollow site over the top site and suggests a 1.67-Å Pd-H bonding distance. No first-principles total-energy calculation has been published for H on Pd(111) based on periodic calculations. The chemisorption on other faces such as (110) and (100) has been the subject of several density-functional approaches,[26–30] but the (111) face has been only studied by embedded atom method (EAM) techniques. These EAM calculations[31–35] yield identical energies for the hcp and the fcc hollow sites, and the subsurface site is found to be even more stable, which does not seem to be in agreement with experimental data. These EAM calculations give a 3% surface contraction for the bare (111) face, which is also at variance with the LEED determination. The palladium hydride has also been studied with the effective-medium theory.[36]

TABLE I. Atomic basis set used in the calculation. Each atomic orbital is described by a numerical atomic orbital (NAO) and/or a Slater-type orbital (STO) whose exponent is given in the table. The frozen core orbitals are not indicated and only described by a NAO.

	Pd					H	
	$4s$	$4p$	$4d$	$5s$	$5p$	$1s$	$2p$
NAO	Yes	Yes	Yes	Yes	No	Yes	No
STO	3.85	3.15	1.5	1.85	1.85	1.28	1.0

The calculation method and the geometrical models for surface and adsorption will be presented in Secs. II and III. Then the results for the interaction of hydrogen with a frozen surface layer will be detailed (Sec. IV). The influence of the Pd first interlayer relaxation will be studied in Sec. V. Finally, in Sec. VI, the electronic structure and bonding of the Pd(111)/H system will be discussed.

II. CALCULATION METHOD

All the calculations performed in this study have been made using the Amsterdam density-functional code for the periodic structures (ADF-Band).[37] This program solves the Kohn-Sham equations[38,39] for a periodic structure in one, two, or three dimensions. Relativistic effects are not taken into account. If not completely negligible, these relativistic effects have been shown to have only small consequences in the case of palladium.[40] The electron wave functions are developed on a basis set of numerical atomic orbitals (NAO) and of Slater-type orbitals (STO). This kind of function describes well the cusp conditions of the atomic orbital. For the core of the heavy atoms (in this case Pd), we use a frozen core approximation to reduce the size of the basis set. A characteristic of this program is to perform numerical integrations for all the matrix elements.[41] The accuracy of the integration in real space and the sampling of the Brillouin zone for the integration accuracy in k space are the two major numerical parameters in the calculation.

At the LDA level, we use the Vosko, Wilk, and Nusair formulas[42] to calculate the exchange and correlation energy. The nonlocal gradient correction (GGA) introduced by Becke[43] for the exchange energy and Perdew[44] for the correlation one has also been used and compared with LDA.

The choice of the basis set is very important for all quantum chemistry calculations. The use of the NAO and STO orbitals, instead of Gaussians, allowed us to reduce the size of this basis, which increases the computational efficiency of the calculation. The Pd atom is modeled by a frozen core only up to the $3d$ orbital, and all the orbitals up until this one are described by a NAO. Each orbital in the valence shell ($4s$,$4p$,$4d$,$5s$) is represented by a double basis including a NAO and a STO (see Table I). The $5s$ NAO comes directly from the starting configuration of the atom, which we have

chosen to be $4d^9 5s^1$. This configuration improves the quality of the basis, but has no influence on the final solution, when the convergence is reached. We have also introduced a $5p$ STO as a hybridization function on the Pd atom. The hydrogen atom is represented by the same kind of basis set, including a NAO and a STO for the $1s$ and a STO $2p$ for the polarization. It has been shown that this kind of basis is large enough to investigate the adsorption of hydrogen on a metallic surface.[45] The use of NAO's in the basis set is also efficient in reducing the basis set superposition errors since the isolated atoms are quite well described. The ADF code uses an auxiliary basis to fit the electronic density. A large set has been used here in order to achieve a good accuracy. For the palladium atom, the fit basis includes 60 STO's $(21s,13p,12d,8f,6g)$ and for the hydrogen, we use 17 STO's $(7s,4p,3d,2f,1g)$.

On a more technical field, all the calculations are performed with an integration accuracy greater than 10^{-4} and at least 15 k points in the reduced Brillouin zone for all the two-dimensional (2D) cells. Some more accurate tests on those parameters show a very small deviation of the energy, and suggest that in this case, the numerical accuracy of the program is around 0.02 eV, not including the systematic deviation due to density-functional approach.

III. DESCRIPTION OF THE MODEL

The choice of periodic calculations allowed us to study the adsorption of hydrogen at nonzero coverage, which is very important for the catalytic point of view. The real conditions of the reaction involve normal or high pressure in hydrogen. In order to be close to the catalytic conditions, it is more reliable to take in account the incidence of the high coverage on the surface. The goal of the study is to investigate the behavior of a hydrogen atom overlayer on a (111) palladium surface. The surface itself is modeled by a slab, that is a solid, infinite periodic in two dimensions, and composed of a given number of layers in the other one. We label this dimension Z and the two others, representative of the infinite surface, X and Y. In our model there is no periodicity at all in the Z direction, so we do not have to check the influence of one slab on another. Now that we have defined the surface, we will describe the different adsorption sites and the different coverages. We chose to chemisorb hydrogen on only one side of the slab. By convention the origin of the Z coordinate is positioned on the plane defined by the cores of the uppermost palladium layer, so the positive Z are above this plane, that is to say outside of the slab, and the negative part of the axis is inside the bulk. The geometry of the (111) surface leads us to define five different sites of adsorption for the H atom (see Fig. 1). They are classified by increasing number of H-metal bonds: (1) The top site, just above a Pd atom of the first layer, (2) the bridge, where the H is between two Pd atoms, (3) and (4) the two threefold hollow sites: the hcp one, where there is one Pd atom just below the H in the second layer, and the fcc one, for which there is no palladium atom below. (5) The last site (subsurface) is inside the slab, corresponding to a negative Z, between the first and the second layer, in a threefold cavity. Only the octahedral subsurface site, which is right below a fcc hollow site, was considered since the tetrahedral site is known to be less stable. For each of those sites, we have studied the influence of the coverage with two different H arrays in relation with two ordered structures found by LEED. The first one is a 1×1 surface, implying that there is one H adatom for one Pd atom on the first layer (coverage 1). The second one is a $\sqrt{3}\times\sqrt{3}$ surface with one H in the unit cell for three metallic atoms (coverage $\frac{1}{3}$, Fig. 1).

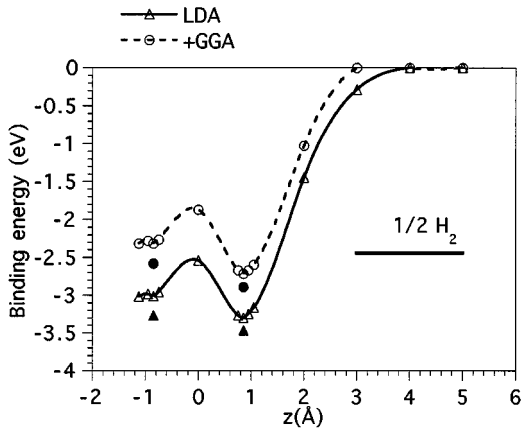

FIG. 2. Potential energy curve for a displacement of H perpendicular to the Pd(111) surface at an fcc hollow site. Calculations with LDA (triangles, full line) and GGA (circles, dashed line) exchange-correlation functionals are indicated. The white (black) symbols correspond to a coverage of 1 ($\frac{1}{3}$). The half H_2 dissociation energy, which is the limit for a stable adsorption, is given. The Pd(111) surface is represented by a frozen three-layer slab with a Pd-Pd distance of 2.75 Å.

IV. RESULT FOR THE HYDROGEN ADSORPTION ON A FROZEN Pd(111) SURFACE

For each of the previous sites, we performed an optimization in Z to determine the adsorption geometry. This optimization is made on a three-layer slab, and for a coverage of one (one H per Pd atom). The H binding energy is defined by the reaction $H+S \rightleftarrows H_{ads}$, where S represents the surface, while the adsorption energy is defined by the reaction $\frac{1}{2}H_2+S \rightleftarrows H_{ads}$. The adsorption is stable only if the binding energy is greater than 2.44 eV at the LDA level and 2.43 eV at the GGA level. For the H atom the total energy for the LDA level is -13.02 eV, 0.58 eV higher than the GGA result (-13.60 eV), which is very close to the experimental value. The same trend appears for H_2 for which the energy difference is 1.11 eV, therefore yielding a similar H_2 formation energy for the two functionals. The H_2 molecule is therefore a special system since the bond energy is not reduced when going from LDA to GGA.

In this part, no relaxation of the Pd surface will be considered: it will be frozen at the bulk termination geometry, with the experimental Pd-Pd distance (2.75 Å). Let us first discuss the (1×1) overlayer of fcc hollow sites on a three-layer slab (Fig. 2). In this case we find two maxima in the Z direction. The most stable one is above the surface. It gives a Pd-H distance of 1.80 Å, and it corresponds to a binding energy of -3.24 eV at the LDA level and -2.65 eV at the GGA one. The second minimum is inside the slab. In this situation, the Pd-H distance is 1.80 Å too (first layer Pd) and

TABLE II. Optimal H height (Å, relative to the first metal layer), Pd_1-H distance (Å), and H binding energy (for the LDA and the GGA functionals) for the frozen three-layer slab as a function of the binding site.

	Hollow fcc	Hollow hcp	Bridge	Top	Subsurface
z (Å)	0.85	0.90	1.0	1.57	−0.85
$d(Pd_1\text{-H})$ (Å)	1.80	1.83	1.70	1.57	1.80
E(LDA,eV)	−3.24	−3.08	−3.11	−2.57	−2.97
E(GGA, eV)	−2.65	−2.48	−2.54	−2.07	−2.28

the adsorption energies are −2.97 eV (LDA) and −2.28 eV (GGA). The (1×1) array of H atoms in subsurface sites is therefore only stable with respect to $\frac{1}{2}H_2$ at the LDA level. For this unrelaxed calculation the barrier for penetration in the bulk is rather high (0.5 eV LDA and 0.47 eV GGA) and this point will be discussed in more detail later. The perpendicular vibration for the surface fcc hollow site was determined by fitting a Morse curve to the associated part of the potential. The result frequency is 1250 cm^{-1}, 25% higher than the experimental value[18] and comparable to the calculated determination on a Pd cluster[21] (1100 cm^{-1}). The variation might be explained by a different coverage situation. The LDA and the GGA determinations of this vibrational state lead to a similar result.

We performed the same optimization for the other sites and the conclusions, relative to the distances and the binding energies, are summarized in Table II. The most stable site at the GGA level as well as at the LDA one is the fcc hollow site. The bridge site and the hollow hcp one lead to a similar binding energy, so the energetic ordering of these sites is not completely clear-cut at this point due to the limited number of layers. The important point is that the hcp hollow site is significantly less stable than the fcc one (0.17 eV). This is in contrast with the EAM results but agrees with the experimental data. The situation concerning the two less stable sites is much more clear, and we deduce that the top site is the most unfavorable one and it corresponds to an unstable adsorption. For all the situations, the differences between the energies, regarding the functional approximation viewpoint, is in the same range: the LDA calculations overestimate the binding by 0.6–0.7 eV. This reduction of the bond energy at the GGA level is a general phenomenon, if H_2 is excluded as previously mentioned, since the GGA energy lowering is smaller in the adduct than in the separated fragments, because the density gradient is weaker in the bond region. This bond energy variation is very similar to the difference between LDA and GGA H atomic energies. However, this seems to be a coincidence and it would certainly be oversimplistic to assume that all the LDA error is concentrated in the H atom itself. Despite this bond energy difference, the two approximations lead to quite the same Pd-H distance for all the sites [for example, 1.79 Å (LDA) and 1.80 Å (GGA) for the fcc site].

Even if the description of the adsorption seems to be satisfactory, it is necessary to test the influence of the parameters of the system on the results. The most important one is the number of layers that we use in the slab, to describe an infinite solid. So the binding energy for the five sites was studied as a function of slab thickness, from one to five layers (Fig. 3). The optimum geometry obtained with the three-layer slab was used in each case. The variation of the optimum geometry with slab thickness was tested for the fcc hollow site and for one, two, and three layers. The height difference was found to be very small (0.02 Å between two and three layers). The stability order of the site does not depend on the number of layers, except for the hcp hollow–bridge energies that are very close and that are not easily positioned one relative to the other. On a more quantitative side, the convergence of the energy with the number of layers is slightly oscillatory but fast and even a slab with two layers gives reasonable results. We can conclude that we have approximately reached the convergence concerning this parameter, and that the three- and the four-layer slabs already give a rather accurate description of the binding energies and of the electronic properties. A more detailed study of the Pd-H electronic interaction in Sec. VI will underline this point. Some previous works[45,46] on the adsorption of H or other adsorbates metal surfaces also led to the point that a three-layer slab is large enough and that even a totally frozen electron description for the third-layer atoms induces only small variation on the description of the chemisorption. The second important computational parameter is the Brillouin zone sampling. A test for the fcc hollow site with a larger number of k points, 28 instead of 15, only gives a 0.02-eV variation in the binding energy.

From those values, we can estimate the diffusion barrier of the H adatom on the Pd(111) surface. We consider two hypothetical diffusion paths on the surface (Fig. 4). The lowest-energy path goes from one hollow fcc site to another, through bridge and hcp hollow sites, and yield a diffusion barrier of 0.15 eV at the GGA level, which is lower than the EAM determination[31–35] (0.2 eV) even if in our case no relaxation is allowed. This suggests a very fast diffusion of the

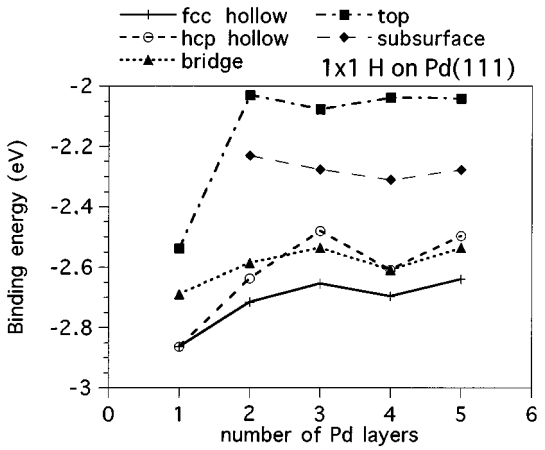

FIG. 3. H binding energy (eV) for each site as a function of the number of layers. The GGA functional and the optimal geometry of H on the three-layer slab are used.

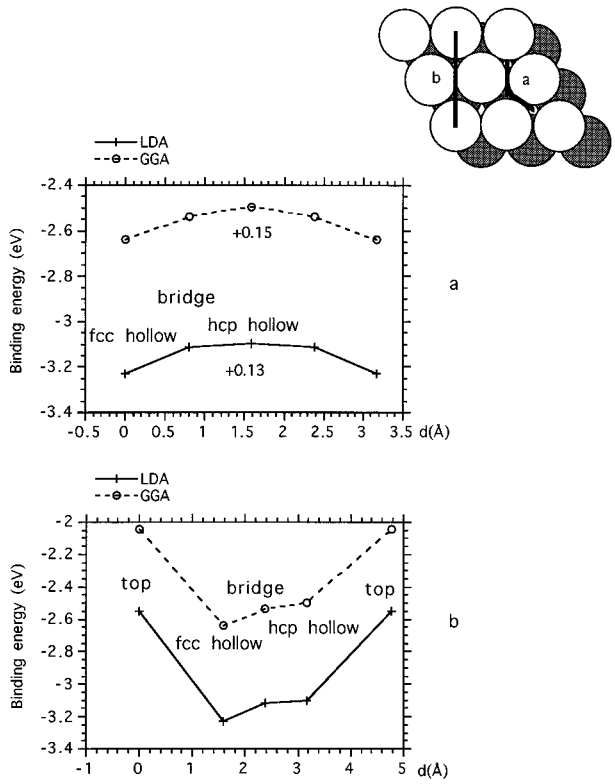

FIG. 4. H binding energy along two possible paths for the H surface diffusion on a five-layer slab. The LDA (solid line) and the GGA (dashed line) functionals are given.

H adatom on the metallic surface, in agreement with the experimental data. It does not seem possible to use a classical treatment for the diffusion process due to the low value of the calculated barrier.[6]

The last point studied on the frozen surface is the influence of the coverage on the adsorption energy. The first calculations are made in a high coverage situation ($\theta=1$). So, we study the same sites for a smaller coverage of $\frac{1}{3}$ ($\sqrt{3}\times\sqrt{3}$ structure). The unit cell includes three palladium atoms on each layer and the calculations are very CPU time consuming, so the Pd-H bond distances were not optimized. We used the H height optimized for the (1×1) overlayer, and a two-layer slab (that is, a cell of six Pd and one H). For all the sites, the binding energies increase with decreasing coverage (Fig. 5) but the stability order of the various sites is kept identical, and the most stable site is always the fcc hollow one. The difference in the adsorption energy is quite site insensitive (0.15–0.22 eV). If we compute the direct H-H repulsion for a 1×1 and a $\sqrt{3}\times\sqrt{3}$ structure of H atoms (without the Pd surface), we find a difference of 0.2 eV, a value comparable with the variation of the adsorption energy. So a great part of this variation can be attributed to the direct H-H repulsion. The computed values for coverage $\frac{1}{3}$ are also relevant in the limit of the very small coverages (experimental data and EAM calculations show little variation of the adsorption energy and of the work function below a coverage of $\frac{1}{3}$). Another important effect appears for this coverage. Since all the sites are more stable, the subsurface one becomes stable toward the H_2 gas phase molecule at the GGA level, since the binding energy increases from -2.31 to -2.58 eV and goes beyond the -2.43-eV limit. This fact is in agreement with the experimental stability of the subsurface site.

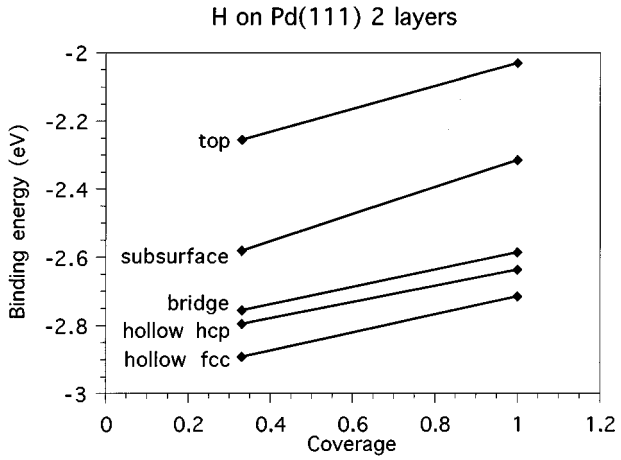

FIG. 5. GGA H binding energy for two coverages ($\frac{1}{3}$ and 1) on the two-layer slab.

Therefore we can conclude that the calculation at the GGA levels gives an adsorption energy in very good agreement with available data. The experimental adsorption energy is -0.45 eV for coverages between 0 and $\frac{1}{3}$, while the calculated value for the $\frac{1}{3}$ coverage at fcc hollow sites is -0.46 eV. The optimum structure is the fcc hollow site, the hcp one and the bridge site being 0.15 eV less stable. The subsurface site is also stable at low coverage but somewhat less than the surface sites, with an adsorption energy of -0.15 eV in good relation with experimental values (-0.1–0.2 eV). On the contrary, results at the LDA level significantly overestimate the adsorption energy ($\sim$0.6–0.7 eV). The calculations with cluster models[19–21] of the surface tend to add an additional binding energy increase, unless very large clusters are used. Such a good agreement between GGA chemisorption energies and experimental data has already been noticed for CO adsorption on Cu.[47] The results contrast with EAM calculations,[31–34] which give an identical energy for both hollow sites with a subsurface site even slightly more stable, and with embedded cluster calculations[22] that favor the bridge site by 0.2 eV.

V. HYDROGEN ADSORPTION ON A RELAXED Pd(111) SURFACE

All the previous calculations have been performed on a frozen Pd surface. We have supposed that the interlayer distance at the surface in the slab was the same as the one in the bulk. It is well known experimentally that the palladium (111) surface presents only a very small outward relaxation of the first interlayer spacing (about $1\%\pm2.5\%$). The effect of this small geometric modification also should be small on the binding energies and the order of the sites should be unaffected, but the chemisorption of hydrogen might result in a significant adsorbate-induced relaxation. In order to understand the influence of the surface relaxation on the binding energies and on the electronic properties, we let the Pd(111) first surface interlayer relax, keeping the other layers frozen. This influence of the relaxation is believed to be

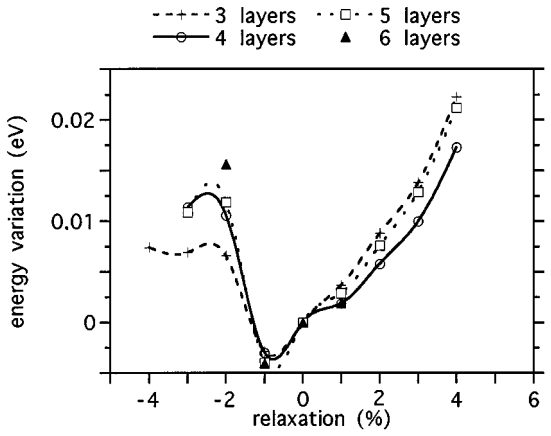

FIG. 6. Influence of the z relaxation of the surface layer, for three- and six-layer slabs, in the case of the bare surface (GGA).

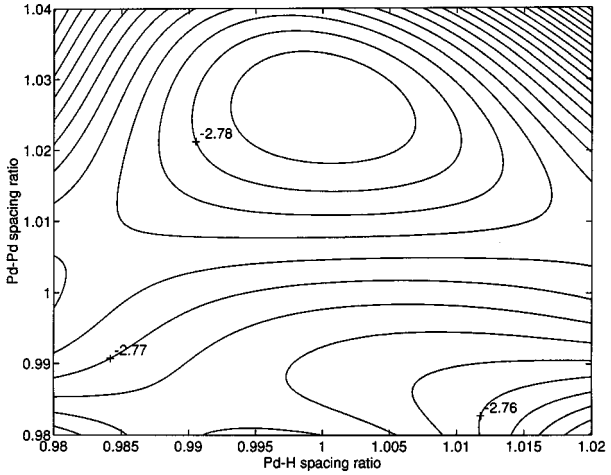

FIG. 7. GGA H binding energy for the fcc hollow site as a function of H-Pd_1 and Pd_1-Pd_2 interlayer spacings. The interlayer spacings are relative to the unrelaxed situation (H-Pd_1: 0.85 Å; Pd_1-Pd_2: 2.34 Å).

rather small due to the close-packed nature of the (111) surface, but to our knowledge, nobody really investigated this phenomenon, using first-principles methods.

The previous part of the study demonstrated that the GGA calculations give much more accurate H binding energies compared with LDA. Therefore this relaxation study will be performed at the GGA level. The first step is to optimize the Pd-Pd distance in the bulk at this level of approximation. The result is 2.86 Å, which overestimates the experimental one by 2.8%. This overestimation is only partly corrected by the addition of $4f$ orbitals in the basis, but this improvement is not determinant and it increases the computational effort, so we decided to keep the previous basis set and to use the distance of 2.86 Å as our bulk optimum one. Notice that, with the same basis set, the LDA calculation gives a 2.75-Å optimum, in perfect agreement with the experiment, but with a strongly overestimated H adsorption. From this point, we let the first layer relax, keeping all the other ones fixed. We first completed this investigation for three- to six-layer bare slabs (Fig. 6). This series of slabs is very consistent with an inward relaxation of less than 1% (0.6%) as a limit result. Even the three-layer slab gives a good result. For all the slab studied, the second layer was kept fixed. This approximation should not have any large consequence. Indeed, the relaxation of the second layer is always smaller than the relaxation of the first one, because it has an environment similar to that of the bulk. Therefore, from these calculations, the Pd(111) surface shows almost no relaxation compared to the bulk termination. This contrasts with the general situation of metal surfaces, which usually gives an inward relaxation of a few percent. An explanation of this limited palladium relaxation will be given in Sec. VI.

For the surface with a (1×1) H adsorption, in order to be able to simultaneously optimize the H and surface Pd atom heights, we had to limit the model to a three-layer slab. Such a number of layers yields a reasonable accuracy for the adsorption of the hydrogen on the surface as well as for the bare surface relaxation. This influence of the relaxation will be checked for the most stable surface and subsurface sites. If the surface is frozen, the change of the cell parameter from the experimental 2.75 Å to the calculated optimum 2.86 Å gives only a small change for the fcc hollow site energy (from -2.65 to -2.77 eV). However, the increase of the subsurface site binding energy is more significant (from -2.28 to -2.62 eV). This effect is certainly due to a release of the H-H and H-Pd electronic repulsion with a larger Pd-Pd distance, especially for the subsurface site. Starting from that point the two-parameter optimization of the hollow fcc site (Fig. 7) shows only a small effect on the binding energy, which goes from 2.77 to 2.78 eV. On the geometric point of view, the differences are also small. The optimum of the two parameters (the hydrogen-adlayer–first-palladium-layer distance, and the first to second palladium layer distance) are 0.85 and 2.40 Å. Therefore the Pd-H distance is not affected by the relaxation, while the Pd surface interlayer spacing expands by 2.7% compared to the bulk value (2.34 Å for a Pd-Pd distance of 2.86 Å).

For the subsurface site, the potential energy surface (Fig. 8) is more complicated. The relaxation increases the optimum binding energy in a more significant way (from

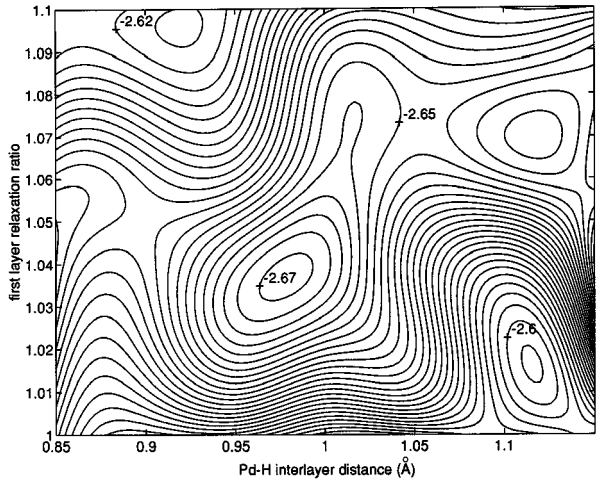

FIG. 8. GGA H binding energy on the subsurface site as a function of H-Pd_1 and Pd_1-Pd_2 interlayer spacings. The Pd_1-Pd_2 interlayer spacing is relative to the unrelaxed situation (2.34 Å).

TABLE III. Adsorption energy (eV) for the best surface site and for the subsurface site, for two different coverages (θ).

	Frozen surface		Relaxed surface		Experimental
	$\theta=1$[a]	$\theta=1/3$[b]	$\theta=1$[c]	$\theta=1/3$[b]	Low coverage
Hollow fcc	−0.27	−0.46	−0.35	−0.53	−0.45
Subsurface	+0.09	−0.15	−0.24	−0.42	−0.2[d]

[a]Four-layer slab.
[b]Two-layer slab, using optimal geometry of the $\theta=1$ calculation.
[c]Three-layer slab.
[d]Experimental values for the H adsorption in the Pd bulk and not for the subsurface site.

−2.62 to −2.67 eV) but the surface is very flat and different coordinates correspond to very similar energies that would yield a very large vertical position disorder for the subsurface H atom (in agreement with the LEED study). The ''optimum'' corresponds to the H atom being 0.98 Å below the Pd surface atom with a 3–4 % outward relaxation of the surface Pd layer. However, there is a second minimum and a complete range of positions in between which energies are only higher by less than 0.01 eV (beyond the precision limit of the calculation). This second optimum corresponds to a H atom 1.12 Å below the surface (which is very close to the layer middle) and to a 7% Pd interlayer expansion. Therefore, due to the very flat nature of the potential, it is not possible to precisely conclude on the geometric position of the optimum.

If we consider the barrier for going from the surface fcc hollow site to the subsurface octahedral site, the fact of slightly increasing the Pd-Pd distance from 2.75 to 2.86 Å already yields a reduction of it, even without inclusion of the relaxation, since it goes from 0.47 to 0.34 eV. Allowing the first surface metal interlayer spacing to relax only slightly modifies this value (0.33 eV) and this interlayer is increased by 5% when the H atoms are within the first Pd layer, at the barrier maximum position. It should be noted that this barrier corresponds here to a simultaneous penetration of a 1×1 H array. There is no experimental determination of the H penetration barrier on the (111) face to our knowledge. The only experimental value is the diffusion barrier within the bulk (0.23 eV). This barrier is calculated to be 67 meV with EAM.[34]

Taking into account the surface relaxation with GGA calculations therefore requires using a slightly expanded bulk distance, which has non-negligible consequences on the H binding energies, while the relaxation itself has only a minor influence on the energetic results, with only a slight expansion of the first interlayer spacing upon H adsorption. With the expanded lattice, the electronic repulsion is decreased, especially for the subsurface site, and the energy difference between surface and subsurface adsorption is reduced to 0.11 eV, the surface site still being the most stable one. The penetration barrier is also diminished to a more reasonable value, if we compare with the bulk diffusion barrier.

The calculations with the relaxed surface hence lead to a slightly stronger binding compared to the 2.75 Å Pd-Pd distance frozen case, mainly because of the expanded bulk Pd-Pd distance (2.86 Å) (see Table III for a summary of adsorption energies). This is especially true for the 1×1 structure where the H atoms feel a significant mutual repulsion. If we use this relaxed optimal geometry with the $\frac{1}{3}$ coverage model on a two-layer slab, the difference with the frozen case is less important and the adsorption energy for the surface fcc hollow site is −0.53 eV (to be compared with the −0.45-eV low coverage experimental value), while it is −0.42 eV for the subsurface octahedral site. There is no experimental value for this adsorption energy of the subsurface site, but this site is known to be slightly more stable than the bulk adsorption case (−0.2 eV). Our calculations are not in complete agreement with the EAM results, since in our case the surface site is 0.1 eV more stable than the subsurface one, in contrast with the EAM where the subsurface case is favored with a very small difference between the two.

VI. ELECTRONIC STRUCTURE

In order to understand the chemical binding, the electronic effects that govern this adsorption must be investigated. The influence of the H atom on the metal electronic structure and the nature of the metal-hydrogen bond have been analyzed with a Mulliken approach, on the basis of the local density of states (LDOS) and crystal orbital overlap population (COOP) curves obtained with a four-layer slab model.

The LDOS on the surface atom and subsurface atom for the bare slab of four layers are shown in Fig. 9. The *d* band is clearly visible and it is slightly more narrow for the sur-

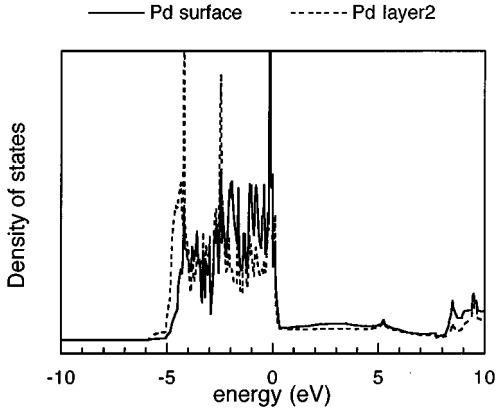

FIG. 9. DOS of the bare four-layer slab projected on the surface (solid line) and subsurface (dashed line) Pd atoms. The energy axis is relative to the Fermi level.

TABLE IV. Mulliken electronic populations for the H atom, the first (Pd_1) and second (Pd_2) Pd layer atoms for a four-layer slab, the Pd in the bulk, in the case of the separated entities and the fcc hollow chemisorption.

	H	$Pd_1(sp)$	$Pd_1(d)$	$Pd_2(sp)$	$Pd_2(d)$	Bulk(sp)	Bulk(d)
Separated	1	0.79	9.20	0.91	9.10	0.89	9.11
fcc hollow	1.14	0.77	9.04	0.91	9.11		

face atom that has a reduced coordination (9 instead of 12). On the contrary the LDOS is enhanced at the surface for nonbonding states near the band middle. The energy scale is relative to the Fermi level E_f, which is positioned near the top of the *d* band. The charge transfer to (or from) the surface is roughly zero (0.008 electron), the surface atom having the same charge as the bulk one. For the five- and six-layer slabs, the charge on the third-layer Pd atom is exactly zero, and even more, the *sp*-*d* electron distribution is the same as that of the bulk. However, the distribution of electrons into *d* and *sp* levels is modified at the surface, even if the total charge is not. Indeed, due to the narrower *d* band, the *d* occupation is enhanced at the surface (+0.09 electron) but this is compensated by a reduced *sp* occupation (−0.09 electron, see Table IV). This intra-atomic redistribution at the surface plays an important role for the relaxation process.

Figure 10 shows the total density of the slab with a 1×1 H overlayer for the different sites that we considered. A new peak is present below the *d* band compared with the bare surface. This peak is located at a forbidden energy for the bulk: it corresponds to a well-known surface state (also called split-off state) induced by the H adsorption. This feature was already studied in detail by Louie and co-workers.[23,24] The peak position is clearly dependent on the H binding site, the gap between the surface state, and the *d* band increasing with larger H-surface coordination. For the subsurface site it is positioned 8 eV below E_f and 6.4 eV below E_f for the fcc surface site. If less coordinated sites are considered, the peak gets closer to the *d* band bottom, and it is inside the *d* band for the top site for which the split-off state has disappeared.

The LDOS on the surface and subsurface Pd layers and on the H atom are given in Fig. 11. The H 1*s* orbital is mostly present in the split-off state, where it mixes with the first-layer Pd orbitals. The Pd-H mixing within the *d* band is very small. The first-layer Pd has a significant weight in the split-off state, but this weight decays very quickly in the layers below (it is already very small on the second layer) as it should be for a localized surface state. The fact that the Pd-H interaction is mostly represented by this split-off state explains the rather fast convergence of the binding energy with slab thickness: the H atom is only weakly present in states that propagate inside the bulk. The band structure of Fig. 12 clearly shows the dispersion (1.60 eV) of the split-off state below the surface *d* band. The dispersion of this split-off band has been studied experimentally.[25] This band is 7.9 eV below E_f at the Γ point of the Brillouin zone, 6.4 eV at *M*, and 5.9 eV at *K*. The calculated results are, respectively, 7.5, 6.6, and 5.9 eV for these *k*-space positions in the case of the hollow site, which is in good agreement (both for the dispersion and the precise band shape) and indicates a reliable description of the electronic structure with this calculation method. As already noticed by Louie and co-workers,[23,24] this study of the band structure is another indication that the most stable adsorption site is indeed the surface fcc hollow one, and not the subsurface site.

Figure 13 decomposes the LDOS for the associated peak on the atomic orbitals of the first-layer Pd atom. The lowest part of the peak corresponds to the area around the Γ point in the band: there, the H atoms are in phase in the 2D Bloch function and this implies for symmetry reasons that only the *s* and dz^2 Pd orbitals can interact with the H atom (see Fig. 14). The dz^2 orbital only interacts weakly with the H, because the H is more or less positioned within the nodal cone of that *d* orbital, and therefore only the *s* orbital significantly contributes to that low-energy part of the peak. On the contrary, the highest part corresponds to points in *k* space close to the Brillouin zone edge where neighboring H atoms are out of phase in the wave function (Fig. 14), which means that only the *d* orbitals with a nodal plane perpendicular with the surface can interact (dxy, dx^2-y^2, dxz, dyz). This interaction, which creates the highest part of the peak, clearly demonstrates and confirms the participation of the Pd *d* orbitals to the Pd-H bond, the electronic charge of the *d* orbitals in the peak being indeed much larger than the *s* electronic charge.

The total atomic charges of the H and the three first Pd layers are represented in Fig. 15 for the case of the 1×1 adsorption on a four-layer slab. The charge on the H atom is strongly dependent on the adsorption site and it approximately correlates with the position of the split-off state in the spectrum. The charge is more negative when the split-off state is low in energy (subsurface site) because in that case the peak, being more detached from the *d* band, has a larger weight on the H atom. For the hollow and bridge site, the negative charge is smaller and the H atom is almost neutral, meaning that the split-off state has a more balanced Pd-H character. The Pd atom of the first layer has on the contrary a small positive charge, which, however, does not match exactly the opposite charge of H. The second and third Pd layers are almost neutral, while the fourth layer of the slab plays the role of an electron reservoir and ensures the final charge neutrality of the slab. In the case of the most stable fcc site, the H atom has a −0.13 charge, while the first-layer Pd has a charge of +0.17. Compared to the bare surface, the *d* population is reduced by 0.16*e* while the *sp* population is almost unchanged (Table IV).

In order to go beyond the LDOS analysis and to understand the Pd-H and Pd-Pd bond strength, COOP curves have been calculated. These curves represent the DOS(E) weighted by the overlap population in the wave function at energy E between two atomic orbitals or two atoms. So we can decompose the interaction in bonding (positive value), antibonding (negative value), and nonbonding energy re-

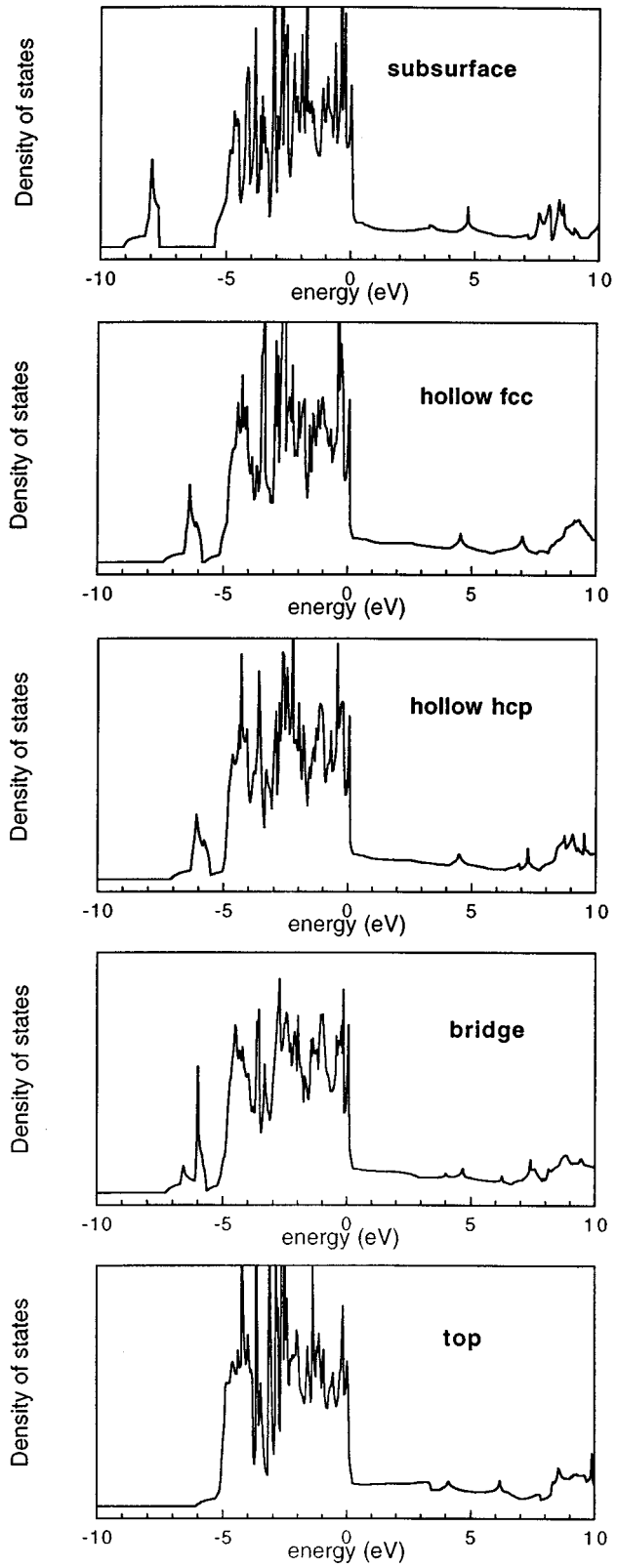

FIG. 10. DOS of the four-layer slab with a (1×1) H overlayer for the five different sites. The structures correspond to those of Fig. 3. The energy axis is relative to the Fermi level.

gions. The integral up to the E_f represents the overlap population and so gives an indication of the bonding character of the considered interaction. The COOP curves for the Pd-H bond are shown in Fig. 16. The Pd atom can be considered

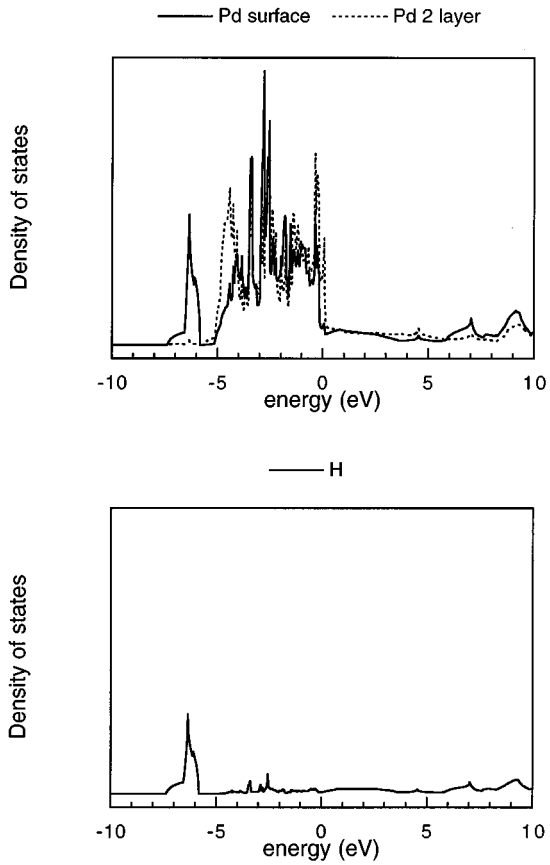

FIG. 11. DOS of the four-layer slab with a (1×1) H overlayer in the fcc hollow site projected on the H atom (bottom), the Pd surface atom (top, solid), and the Pd subsurface atom (top, dashed).

with all its orbitals (atomic COOP, top), or the contribution of *sp* (middle) or *d* (bottom) orbitals can be extracted. These curves underline again the importance of the split-off state that contains most of the Pd-H bonding effect. In the total COOP, all levels up to the Fermi energy correspond to a bonding situation, but the *d* band region is almost nonbonding. The Pd-H overlap population is 0.69, and it is already

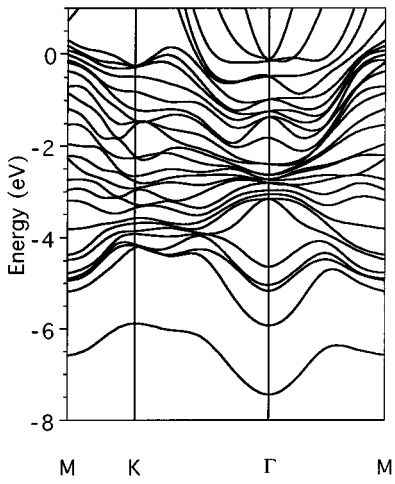

FIG. 12. Energy band diagram for the five-layer slab with a (1×1) H overlayer in the fcc hollow site.

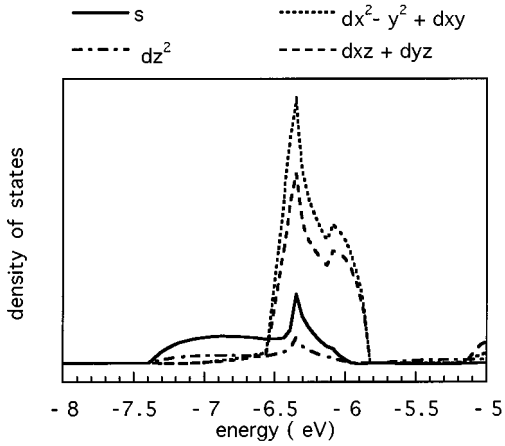

FIG. 13. Decomposition of the split-off band on the contributions of the surface Pd atomic orbitals for a (1×1) H overlayer in the fcc hollow site.

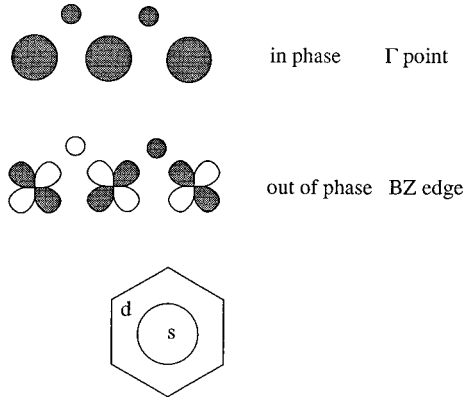

FIG. 14. Schematic orbital scheme for the split-off state and preponderant Pd atomic orbital contribution as a function of the chosen *k*-space position in the Brillouin zone (see text).

0.53 if only the peak of the split-off state is taken into account. The contributions of the *sp* and *d* orbitals of Pd in the overlap population are rather balanced (*sp*: 0.32, *d*: 0.37), which underlines again the importance of the *d* orbitals in the adsorption. The *d* orbitals show a large bonding contribution of 0.34 in the top part of the split-off state (see previous discussion), while the interaction becomes slightly antibonding near the top of the *d* band. For the *sp* orbitals the contribution of the surface state is 0.19, but the interaction remains bonding up to 2.5 eV above the Fermi level. It should be noted, however, that the contribution of the *sp* orbitals is almost equal to that of the *d* orbitals in the COOP, even if the weight of the *sp* states in the split-off band is much smaller. This is due to the better overlap between H(1*s*) and Pd(*sp*) because of their more diffuse character. Therefore the possible conclusion from the LDOS curves alone (Fig. 13) that the *d* orbitals would largely dominate the Pd-H bonding on the metal side is erroneous.

The second bond that is interesting to analyze with the COOP curves corresponds to the interaction between first-layer and second-layer Pd. Let us start with the bare surface, for which this Pd_1-Pd_2 COOP is indicated in Fig. 17 (left column), decomposed in *d/d*, *sp/sp*, and *d/sp* contributions. The *d/d* interaction shows a bonding part, in the bottom of the *d* band and an associated strong antibonding part in the top. Since the *d* band is almost full, these antibonding contributions are occupied so that the *d/d* interaction resembles a 10-electron one and the net result has a slightly antibonding nature. Therefore this *d/d* interaction resembles a 10-electron one and the net result has a slightly antibonding nature. Therefore this *d/d* interaction has a small negative contribution to the Pd-Pd bond (−0.03) and is hence slightly repulsive. This effect is somewhat stronger at the surface, where the Pd *d* population is 0.09 higher for Pd_1, compared to the case of the bulk. One first positive part to the Pd-Pd bond is the *sp/sp* one (0.12) but the major contribution is given by the *d/sp* (and *sp/d*) mixings (0.24), which yield a bonding situation in almost the full *d* band range. The total overlap population sums up to 0.33. The *sp-sp* and *d-sp* interactions are slightly stronger at the surface, which compensates the more destabilizing *d-d* interaction, yielding a very similar bond strength compared to the bulk. Indeed the total overlap population between the second and third layers is 0.32, implying just a very small increase of the Pd-Pd bond at the surface. The interaction with H only slightly changes the Pd_1-Pd_2 COOP curves as shown in Fig. 17 (right column). The split-off state has a minor contribution (+0.05), since its weight on Pd_2 is very small, but the overall result is on the contrary a small decrease of the Pd-Pd overlap population (0.32), matching back the bulk value and implying a very small adsorbate-induced relaxation. The *d/d* interaction is however, slightly less unfavorable since Pd_1*d* population is reduced by the adsorption (see Table IV, it becomes even smaller than the *d* population for the Pd bulk case). This decrease of the *d* population also results in a weakening of the *d-sp* overlap population. The *sp-sp* interaction is slightly increased because of the significant contribution of the split-off state in that case (the small contribution of Pd_2 in the split-off state is mainly *sp*). The overall change in the Pd-Pd bond is dominated by the weakening of the *d-sp* interaction, but this is compensated by the small increase of the *d-d* and *d-sp* bonding. From this conflicting effect, the final change in the bond is only small.

VII. CONCLUSION AND SUMMARY

The adsorption of H on Pd(111) has been studied with density-functional calculations both with LDA and GGA exchange-correlation functionals using the ADF-Band code. The surface is described by a two-dimensional slab with a periodic adsorption of H atoms, comparing for various binding sites a (1×1) structure (coverage 1) with a $\sqrt{3}\times\sqrt{3}$ array (coverage $\frac{1}{3}$). Among the surface sites, the fcc hollow one is found to be the most stable, in agreement with other experimental and theoretical data. The GGA adsorption energy ranges from −0.27 to −0.53 eV, depending on the coverage and on the frozen or relaxed nature of the surface in the calculation (the experimental value is −0.45 eV). The LDA value for the adsorption energy is 0.6–0.7 eV larger in absolute value, yielding an obvious and well-known overesti-

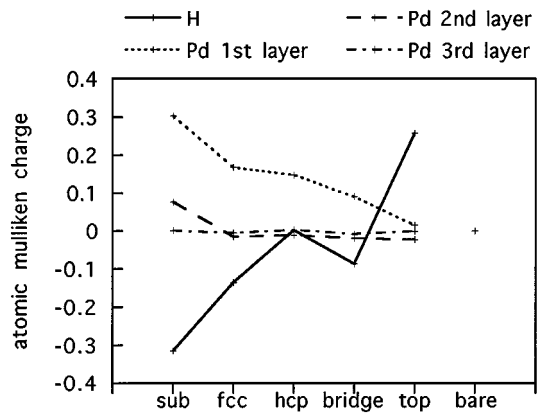

FIG. 15. Mulliken atomic charge for H and palladium atoms (first to third layer) as a function of the adsorption site for a four-layer slab.

mation. The optimal height of the H atom is +0.85 Å relative to the surface Pd layer, very close to the LEED determination.

However, in contrast with EAM theoretical calculations, and in agreement with helium diffraction experiments,[6] the hcp hollow site is significantly less stable (+0.15 eV) than the fcc site and its binding energy is similar to that of the bridge site. The barrier for H diffusion on the surface is then low (0.15 eV). The octahedral subsurface site is stable with respect to H_2, except for the frozen surface with a coverage 1. If the surface is relaxed the subsurface site is only 0.1 eV less stable than the fcc surface site. However, this influence of the relaxation is mostly due to the expansion of the Pd-Pd distance, from the experimental value of 2.75 Å to the calculated GGA optimum of 2.86 Å, the relaxation of the interlayer spacing itself having only a small influence on the energy. For the surface hollow site, the H height is not modified by the relaxation, while the first to second layer Pd spacing expands as expected from the chemisorption, but only by 2.7%. A larger expansion is found for the subsurface site. However, in that case, the energy surface is very flat around the minimum and that expansion and the hydrogen z are not well defined, indicative of a large vertical disorder in that case. The bare surface shows on the contrary no vertical surface relaxation. The penetration barrier from surface to subsurface for a (1×1) array is found to be 0.33 eV if the surface relaxation is included.

Among the parameters of the calculation, the convergence with the number of layers in the slab on the optimum geometry and energy, as well as the convergence with k-space sampling have been tested in detail. For all the sites, a coverage decrease from 1 to $\frac{1}{3}$ rather uniformly results in a 0.2-eV increase of the binding energy.

In the eigenvalue spectrum, a new peak is clearly visible below the Pd band when H is adsorbed and the position of that peak correlates with the H coordination. The dispersion of that H-induced split-off band is in good agreement with photoelectron data. This surface state is mostly localized on the H and first-layer Pd, with a very fast decrease on the subsequent layers, explaining the rather quick convergence

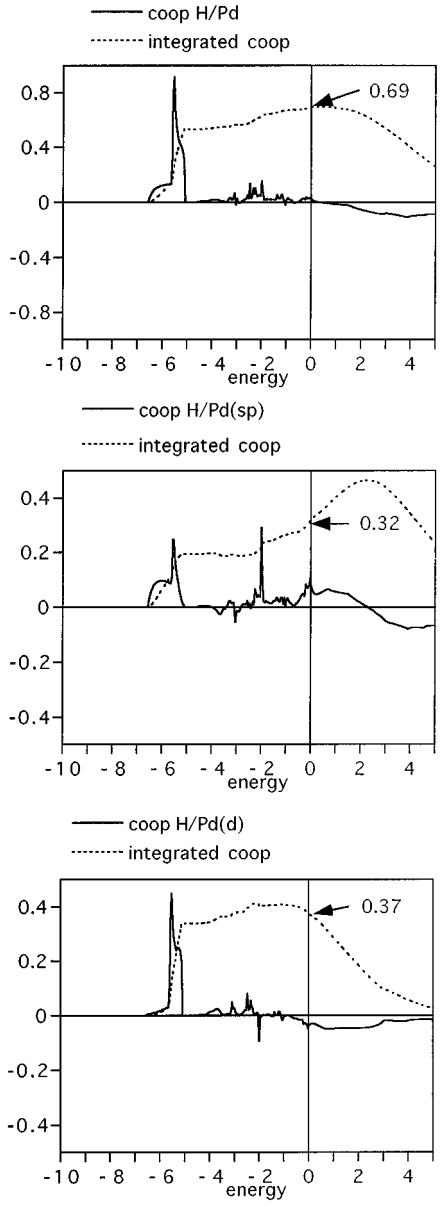

FIG. 16. Crystal orbital overlap population (COOP) for the Pd-H bond (top) with the decomposition on the Pd *sp* (middle) and *d* (bottom) orbitals. The integrated COOP is given for each case by a dashed line and the energy axis is relative to the Fermi level.

of the binding energy with the number of layers in the slab. The contribution of Pd *d* orbitals dominates in that split-off band. The net charge on the hydrogen is small, but depends on the binding site (from −0.3 for the subsurface to +0.25 for the top site). The charge of the surface Pd atom is always positive and small (from +0.3 to +0.03), the difference with the H charge being accounted by the electron reservoir capability of the surface.

The electronic structure has been analyzed in more detail with the COOP curves. They confirm that the predominant Pd-H bonding character is contained in the split-off band with little contribution from the energy levels in the surface *d*-band range but indicate, however, that the *sp* and *d* orbitals

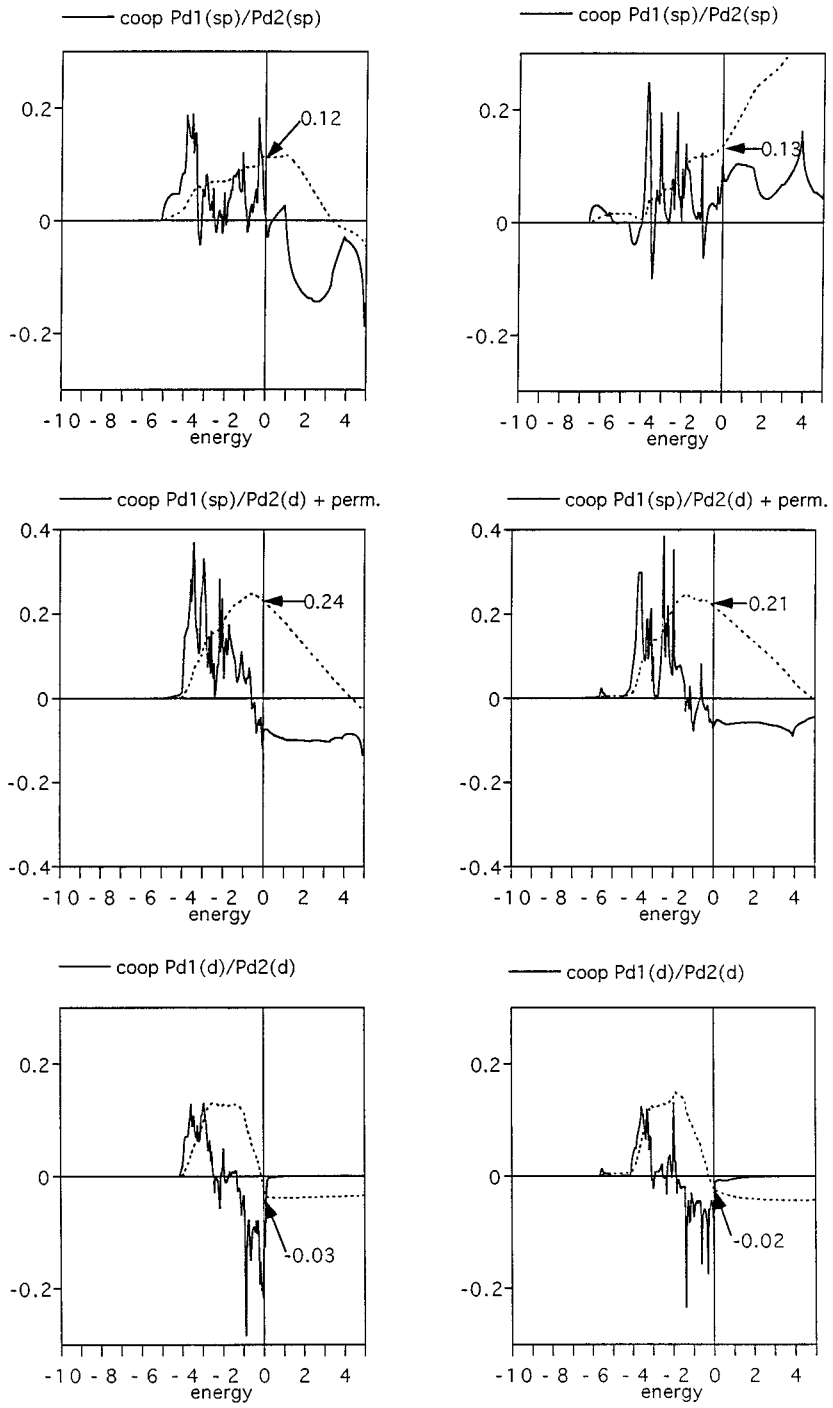

FIG. 17. Crystal orbital overlap population (COOP) between the first- and the second-layer Pd atoms. The bare surface case is given on the left, while the (1×1) fcc hollow adsorption situation is shown on the right. The *sp/sp* COOP is given at the top, while the $sp/d+d/sp$ one is in the middle and the *d/d* one at the bottom. The integrated COOP is given for each case by a dashed line and the energy axis is relative to the Fermi level.

of Pd have a rather equal contribution to the Pd-H bond. The Pd (first layer)-Pd (second layer) COOP shows a net antibonding result of the *d/d* interaction, counterbalanced by a stabilizing effect of the *sp/sp* and *sp/d* ones. Both stabilizing and destabilizing interactions are increased at the surface, resulting in a net very small relaxation. The H chemisorption decreases, the Pd-Pd interaction back to the back value. A similar compensation as before yields a small overall effect, but the net result is a slight weakening of the Pd-Pd bond at the surface. Such an antibonding *d/d* interaction is characteristic of the transition metals with a *d* band almost full. Similarly, small relaxation effects are expected for the other metals in that case, like platinum.

ACKNOWLEDGMENTS

The authors wish to thank G. te Velde and E. J. Baerends for their very valuable help in the use of the ADF-Band code and B. Bigot for helpful discussions. They also want to thank IDRIS at CNRS for the attribution of CPU time (Project No. 940016).

*Author to whom correspondence should be addressed.

[1] T. Ouchaib, J. Massardier, and A. Renouprez, J. Catal. **119**, 517 (1989).
[2] K. Christmann, Surf. Sci. Rep. **9**, 1 (1988).
[3] K. R. Christmann in *Hydrogen Effects in Catalysis, Fundamental and Practical Applications*, edited by Z. Paal and P. G. Menon (Dekker, New York, 1988).
[4] P. Nordlander, S. Holloway, and J. K. Norskov, Surf. Sci. **136**, 59 (1984).
[5] J. W. Davenport and P. J. Estrup, in *The Chemical Physics of Solid Surfaces and Heterogeneous Catalysis*, edited by D. A. King and D. P. Woodruff (Elsevier, Amsterdam, 1989), Vol. 3A, p. 1.
[6] C-H. Hsu, B. E. Larson, M. El-Batanouny, C. R. Willisand, and K. M. Martini, Phys. Rev. Lett. **24**, 3164 (1991).
[7] A. Eaurbach, K. F. Freed, and R. Gomer, J. Chem. Phys. **86**, 2356 (1987).
[8] T. E. Felter, R. H. Stulen, M. L. Koszykowsky, G. E. Gdowski, and B. Barrett, J. Vac. Sci. Technol. A **7**, 104 (1989).
[9] R. J. Behm, V. Penka, M.-G. Cattania, K. Christmann, and G. Ertl, J. Chem. Phys. **78**, 7486 (1983).
[10] Ch. Resch, H. F. Berger, K. K. Rendulic, and E. Bertel, Surf. Sci. **316**, L1105 (1994).
[11] J. Völkl and G. Alefeld, *Hydrogen in Metals I*, edited by G. Alefeld and J. Völkl, Topics in Applied Physics, Vol. 28 (Springer, Berlin, 1978), p. 321.
[12] E. Wilke and H. Brodowsky, *Hydrogen in Metals II*, edited by G. Alefeld and J. Völkl, Topics in Applied Physics, Vol. 29 (Springer, Berlin, 1978), p. 73.
[13] W. H. Mueller, J. P. Blackledge, and G. G. Libowitz, *Metal Hydrides* (Academic, New York, 1968).
[14] K. Christmann, G. Ertl, and O. Schober, Surf. Sci. **40**, 61 (1973).
[15] T. E. Felter, E. C. Sowa, and M. A. Van Hove, Phys. Rev. B **40**, 891 (1989).
[16] H. Conrad, G. Ertl, and E. E. Lata, Surf. Sci. **41**, 435 (1974).
[17] T. Engel and H. Kuipers, Surf. Sci. **90**, 162 (1979).
[18] H. Conrad, M. E. Kordesch, R. Scala, and W. Stenzel, J. Electron Spectrosc. Relat. Phenom. **38**, 289 (1986).
[19] V. Russier, D. R. Salahub, and C. Mijoule, Phys. Rev. B **42**, 5046 (1990).
[20] V. Russier and C. Mijoule, J. Phys. C **3**, 3193 (1991).
[21] A. Rochefort, J. Andzelm, N. Russo, and D. R. Salahub, J. Am. Chem. Soc. **112**, 8239 (1990).
[22] J.-P. Muscat, Surf. Sci. **148**, 237 (1984).
[23] S. G. Louie, Phys. Rev. Lett. **42**, 476 (1979).
[24] W. Eberhardt, S. Louie, and E. W. Plummer, Phys. Rev. B **28**, 465 (1983).
[25] W. Eberhardt, F. Greuter, and E. W. Plummer, Phys. Rev. Lett. **46**, 1085 (1981).
[26] I. Papai, D. R Salahub, and C. Mijoule, Surf. Sci. **236**, 241 (1990).
[27] D. Tomanek, Z. Sun, and S. Louie, Phys. Rev. B **43**, 4699 (1991).
[28] T. L. Einstein, M. S. Daw, and S. M. Foiles, Surf. Sci. **227**, 114 (1990).
[29] S. Wilke, D. Hennig, R. Löber, M. Methfessel, and M. Scheffler, Surf. Sci. **307-309**, 76 (1994).
[30] D. Hennig, S. Wilke, R. Löber, and M. Methfessel, Surf. Sci. **287-288**, 89 (1993).
[31] M. S. Daw and M. I. Baskes, Phys. Rev. Lett. **50**, 1285 (1983); Phys. Rev. B **29**, 6443 (1984).
[32] M. S. Daw and S. M. Foiles, Phys. Rev. B **35**, 2128 (1987).
[33] T. E. Felter, S. M. Foiles, M. S. Daw, and R. H. Stulen, Surf. Sci. **171**, L379 (1986).
[34] S. W. Rick, D. L. Lynch, and J. D. Doll, J. Chem. Phys. **99**, 8183 (1993).
[35] S. W. Rick and J. D. Doll, Surf. Sci. **302**, L305 (1994).
[36] O. B. Christensen, P. Stolze, K. W. Jacobsen, and J. K. Norskov, Phys. Rev. B **41**, 12 413 (1990).
[37] ADF-Band package, Laboratory of theoretical chemistry, Free University Amsterdam (Netherlands); G. te Velde and E. J. Baerends, Phys. Rev. B **44**, 7888 (1991).
[38] P. Hohenberg and W. Kohn, Phys. Rev. **136**, B864 (1964).
[39] W. Kohn and L. J. Sham, Phys. Rev. **140**, A1113 (1965).
[40] S.-C. Chung, S. Krüger, G. Pacchioni, and N. Rösch, J. Chem. Phys. **102**, 3695 (1995).
[41] G. te Velde and E. J. Baerends, J. Comput. Phys. **99**, 84 (1992).
[42] S. H. Vosko, L. Wilk, and M. Nusair, Can. J. Phys. **58**, 1200 (1980).
[43] A. D. Becke, Phys. Rev. A **38**, 3098 (1988).
[44] J. P. Perdew, Phys. Rev. B **33**, 8822 (1986).
[45] G. Wiesenekker, G. J. Kroes, E. J. Baerends, and R. C. Mowrey, J. Chem. Phys. **102**, 3873 (1995).
[46] G. teVelde and E. J. Baerends, Chem. Phys. **177**, 399 (1993).
[47] P. H. T. Philipsen, G. teVelde, and E. J. Baerends, Chem. Phys. Lett. **226**, 583 (1994).